Ultrastructural Characteristics of a Human Sialolith

Hyun-Jin Kim, D.D.S., Soo-Guen Lee, D.D.S., M.S.D.,
Bong-Jik Suh, D.D.S., M.S.D., Ph.D.

Department of Oral Medicine, College of Dentistry and Institute of Oral Bioscience, Chonbuk National University

- CONTENTS -

I. INTRODUCTION

Sialoliths are calcified structures that develop within the salivary ductal system. They are believed to arise from deposition of calcium salts around a nidus of debris within the ductal lumen. This debris may include inspissated mucus, bacteria, ductal epithelial cells, or foreign bodies[1-3]. The small nidus then allows concentric lamellar crystallizations to occur; the sialolith increases in diameter as layer after layer of salts becomes deposited, much like growth rings in a tree[2].

Despite the very extensive literature, the pathogenesis of sialoliths still remains unclear [4-6]. According to Anneroth, it was known that mucoid gel was formed by uniting with mucus, desquamated epithelial cells, inflammatory cells, and sometimes also with the cell membrane and cytoplasm of the disintegrated bacteria and sialolith was made of the salts that deposited on the mucoid gel[4,5]. Harrison reported that the inanimated nucleus was the center of the formation of the sialolith[7]. It was reported by Doku, Berkman and Levy et al that sialolith was formed when calcium was deposited with the altered mucus from sialadenitis[8,9].

Sialoliths most often develop within the ductal system of the submandibular gland; the formation of stones within the parotid gland system is distinctly less frequent[1-3]. The sialoliths are formed more easily in the ductal system of submandibular gland because the submandibular duct is ascending, and furthermore, in contrast to the parotid duct, the orifice of the submandibular duct is considerably narrower, facilitating stasis of the saliva. The non-stimulated saliva from the submandibular gland has a higher mucin content and about twice as much calcium as parotid saliva[3,5,10].

According to Harrison et al, sialoliths occur more commonly in males by a 2:1 ratio[7,10,11]. Sialoliths occur more commonly in males by a

2:1 ratio according to Oh et al in the Republic of Korea[12-15]. There is a interesting report which explains sialoliths are frequently occured in men because of abnormal salivary flow from alcohol drinking and cigarette smoking[16]. Sialolithiasis may occur at any age, but is most common in middle-aged adults[2,3]. According to Oh et al, sialoliths were found in man ranged from 9 years old to 73 years old, but most of sialoliths were found in man ranged from 20 to 60 years old[12-15].

The previous studies of the sialoliths cover from clinical features, diagnosis and treatment of sialolithiasis to composition and structure of sialoliths. There are many reports of clinical cases, but the studies on composition and structure of the sialoliths are rare in Korea[12,13]. Considering that sialoliths may have variable compositions and structures[4-6], and the effects of Extracorporeal Shock Wave Lithotripsy (ESWL)[17-22], new non-surgical therapy for sialolithiasis, are influenced by structure and composition of the sialoliths, the structure and composition of the sialolith should be discussed. Therefore ultrastructural characteristics of a human sialolith which was removed from the submandibular gland duct of a korean female aged 59 years were observed using reflected microscopy and scanning electron microscopy to obtain the fundamental data concerning the management of sialolithiasis.

II. MATERIALS AND METHODS

A sialolith was removed from the submandibular gland duct of a female aged 59 years at the Chonbuk National University Dental Hospital. The removed sialolith was preserved on 0.02% thymol solution. After rinsing it on running water and drying it in the air, it was embedded in acrylic resin to be used in this study. The resin-embedded sample of sialolith was cut into slice 1,000㎛ thickness with a Low Speed Diamond Wheel Saw (SBT, South Bay Technology, U.S.A.). The slice of sialolith was treated with 0.5M ethylene diamine tetra-acetic acid (EDTA) at PH 7.2 for 2 minutes in order to remove a smear layer. The slice of sialolith was observed with a reflected light microscope (SMZ-U, Nikon,Japan), and scanning electron microscope (Hitachi X-650) after coating it with platinum.

III. RESULTS

1. Radiographic features of sialolith

Occlusal radiograph disclosed an oval-shaped radiopaque mass on the ductal area of left submandibular gland (Fig.1).

2. Gross features of sialolith

The removed sialolith was round or oval, yellowish, rough and coarse in surface texture, 14×6×4㎜ in size and 0.5g in weight (Fig.2).

3. Reflected light microscopic features of sialolith

Figure 3 showed an image of the ground section from the cross-sectioned sialolith. The color of the cross-sectioned sialolith was whitish and yellowish. The cross-sectioned sialolith showed central core, lamellar portion which surrounded the central core, and outer surface. Central core was not located at midpoint in the cross-sectioned sialolith but slightly outwardly located. There was a distinctive brown colored border which differentiated between cental core and lamellar portion.

Figure 5 showed an image of a central core of the sialolith. Central core was composed of

bright center and homogenous structure which surrounded it.

Figure 7 showed an image of a middle portion of a central core of the sialolith. The surface of the middle portion of the central core was uneven and irregular.

Figure 9 showed an image of a lamellar portion of the sialolith. There was rhythmical apposition of alternating colors around the central core. It seemed to be rings in a tree.

Figure 11 showed an image of a outer surface of the sialolith. The outer surface was additional and vague in appearance.

4. Scanning electron microscopic features of the sialolith

Figure 4 showed an image of the ground section from the cross-sectioned sialolith. There were concentric and appositional laminations in large portion and there was a homogenous structure in the other part around the central core. The diameters of the cross-sectioned sialolith and central core were approximately 3,500㎛ and 1,500㎛, respectively.

Figure 6 showed an image of the central core of the sialolith. Central core was devided into two parts by the morphologic features. One part was amorphous structure which was located in the middle area of the core and the other part was smooth, latticed structure divided by lines.

Figure 8 showed an image of a middle portion of a central core of the sialolith with amorphous structure.

Figure 10 showed an image of a lamellar portion of the sialolith. There was rhythmical apposition of alternating shells around the central core. And there were crevices between the shells. The thickness of the shell, which was a unit of the lamellar structure, was approximately within 10-40㎛, although the thickness of the shell depended on the site.

Figure 12 showed an image of a outer surface of the sialolith. The outer surface was additional and relatively less demarcated structure.

IV. DISCUSSION

Sialolithiasis is a disease characterized by the formation of calculus inside a salivary duct. Although this condition may arise in any of the salivary glands, there is a tendency for stone to form in Wharton's duct of the submandibular gland. Sialolithiasis may occur at any age, but is most common in middle-aged adults[1-3]. Many reports have indicated that swelling and pain in the submandibular region at mealtimes are the most common symptoms. A decrease of salivary flow is also commonly reported[1-3]. In this study, the age of subject was 59 years old, and her chief complaint was swelling of the mouth floor, but there was no complaint of meal-associated pain. Salivary flow from affected Wharton's duct seemed to be less than that on the normal side.

Sialoliths of the submandibular gland are diagnosed by clinical appearance and radiology[1-3,10,15,17,23,24]. If the sialolith lies close to the ostium or in the middlde third of the duct, it can be palpated in the floor of the mouth. Sialoliths typically appear as radiopaque masses on X-ray examination, although not all stones are visible on standard radiographs, which is perhaps related to the degree of calcification of the lesion. They may be discovered anywhere along the length of the duct or within the gland itself. Sialoliths in the terminal portion of the submandibular duct are best demonstrated with an occlusal radiograph. On panoramic or periapical radiographs, the calcification may appear superimposed on the mandible, and so care must be exercised not to confuse it with an intrabony lesion[1-3,10]. Sialography is the only

imaging modality for examining the fine anatomy of the salivary ductal system and means of ruling out sialoliths[25,26]. Balatt and Rubin had three reasons for sialography: first, to find out the exact location of the sialolith in case of radiopaque sialolith, second, to find out the presence of the sialolith in case of radiolucent sialolith, third, whether there is a constricture in the duct or orifice or not[27]. Additionally, Avrahami persisted that the computed tomography was useful method diagnosing of multiple sialoliths than conventional radiography and sonography[28].

But in this study, there was no necessity to perform the additional examinations for localization of the sialolith, because it was possible to make sure of the presence and location through the clinical and radiologic examinations(panoramic view, occlusal view, periapical standard view).

Many major salivary gland sialoliths can be removed by manual manipulation of the stone through the major duct orifice. When manual maneuvers were failed, a surgical "cut-down" into the main duct is needed. Intraglandular stones, multiple stones within the gland proper, diffuse glandular calcifications, and longstanding obstructions will usually require removal of the stone along with sialoadenectomy[1,2]. Recently, extracorporeal shock wave lithotripsy has been introduced as an alternative treatment of sialolithiasis. Miniature lithotriptors have been developed and show some promise. However, these units are not generally available and their success rates have been variable[17-22].

In this study the sialolith was removed from the duct of the submandibular gland by the sugical cut-down procedure intraorally because of the sialolith was located in the duct of submandibular gland far from the orifice.

Sialoliths vary widely on their size and shape. According to Rauch[10], the weight of most sialoliths lies between 0.1 and 0.3g. Most of sialoliths are round or oval in shape. The surface may be nodular and have angular or pointed projections. The color of the sialoliths ranges from white or yellow to brown[1-3].

In this study, its shape, color and surface show general features as already commented.

Kurachi et al categorized the cross-sectional structure of a sialolith into three parts: a central core, a lamellar portion and an outer surface. He reported that each of the lamellae had almost the same thickness, but the structure was not uniform in that the layers were composed of alternately close and roughly fused granules. He also stated that the outer surface presented a granular appearance[29]. And Morinaga categorized the cross-sectional structures as follows : (A) a sialolith having a relatively small single core and an apparently lamellar structure of concentric layers throughout ; (B) a sialolith having a relatively large single core and lamellar structure mainly at the periphery ; (C) a sialolith having multiple cores and otherwise appearing to be an aggregate of sialoliths ; (D) a sialolith having an almost uniform structure with an only slightly apparent lamellar pattern, otherwise appearing homogenous.

Morinaga, unlike Kurachi et al[29], reported lamellar structures in which each lamella was not even in thickness. And he reported lamellar structures in which lamellae were closely piled upon each other, or roughly pieled up showing crevices. In the closely lamellated structures he also observed board-shaped, needle-shaped or globular crystals[30].

In this study the sialolith was composed of a single central core and lamellar portion and outer surface. The diameter of the central core was the 1/2.5 of the whole sectional diameter.

Inside of the central core was also divided into

two portions. The center of the core seemed to be bright colored surface scooped out irregularly and the surroundings of the center seemed to be dark colored regular surface. The bright center of the core which seemed more brittle than the surroundings was supposed that the center was likely to be partially removed out during specimens prepairing process, and we guess this portion may be the initially formed portion of the sialolith formation. The dark brown line which seemed to be hard crystalline structures distinguished central core from lamellar portions. Lamella portions had almost the stratified shell structuers but in some portions had homogeneous ones. The thickness of the shell, which was a unit of the lamellar structure, was approximately within 10-40㎛, although the thickness of the shell depended on the site. The lamellar structure had crevices located between each layers and so looked friable such as french pastry.

Sialoliths consist of organic and inorganic material whose propotions to each other vary widely. The organic constituents have been less well investigated than the inorganic. They include precipitated mucus, that is, glycoproteins, mucopolysaccharides, cell debris and lipids[1,2,10]. The inorganic components of sialoliths consist of calcium phosphate and calcium carbonate showing the apatitie structure. Studies of sialoliths have mostly involved microradiography, X-ray diffraction and scanning electron microscopy. X-ray diffraction has revealed that the inorganic components which comprise sialoliths include calcium phosphates such as hydroxyapatite, whitlockite, brushite and octacalcium phophate. At least two of these have been found in a single sialolith[4-6,10,31-36]. Yamamoto et al[34] have demonstrated that apatite was frequently observed and that whitelockite was next frequently detected in the sialolith. Brushite and octacalcium phosphate were rarely present in the sialoliths. It was suggested that brushite and weddellite were present in the early stage of sialolith formation and then transformed into the more stable form as apatite. Oh et al[12] demonstrated that the components of sialoliths consist of 38.8% calcium phospate, 33.3% calcium carbonate, 16.6% magnesium phospate and 11.1% magnesium carbonate in 18 cases. X-ray diffraction analysis of the submandibular sialoliths in 26 cases has revealed that a group which had calcium phospate as a major component is 21 cases, a group which had calcium phospate and magnesium phospate as major one 4 cases and ammonium magnesium phosphate group 1 case[13].

This study was designed to observe the ultrastructure of the sialolith using reflected light microscopy and scanning electron microscopy to obtain the fundamental data concerning the management of sialolithiasis, but it is considered that furthermore studies for understanding the chemical component analysis as well as the ultrastructural characteristics of sialoliths from many and various samples should be performed.

V. CONCLUSIONS

The purpose of this study was to evaluate the ultrastructural characteristics of the sialolith. The sialolith was removed from the submandibular gland duct of a korean female aged 59 years by surgical cut-down procedure. The sectioned sialoloth was observed using a reflected light microscopy and a scanning electron microscopy.

The obtained results were as follows :

1. The sialolith consisted of central core,

lamellated shells and outer surface.

2. The central core had a amorphous center.
3. The lamellated shells had concentric laminations in large portion and non-concentric homogenous structure in the other portion around the central core.
4. The diameters of the cross-sectioned sialolith and central core were approximately 3,500㎛ and 1,500㎛, respectively. The thickness of the shell, which was a unit of the lamellar structure, was approximately within 10-40㎛.

REFERENCES

1. Neville B.W. : Oral and maxillofacial pathology. 1st edi., 1995, W.B. Saunders Co., pp326-327.
2. Sapp J.P., Eversole L.R. and Wysocki G.P. : Contemporary oral and maxillofacial pathology. 1st edi., 1997, Mosby-Year Book, Inc., pp 326-328.
3. Shafer W.G., Hine M.K. and Levy B.M. : A textbook of oral pathology. 2nd edi., 1963, W.B. Saunders Co., pp 457-458.
4. Anneroth G., Eneroth C.M., Isacsson G. and Lundquist P.G. : Ultrastructure of salivary calculi. Scand. J. Dent. Res., 86 : 182-192, 1978.
5. Anneroth G., Eneroth C.M. and Isacsson G. : Morphology of salivary calculi. The distribution of the inorganic component. J. Oral Pathol., 4(5) : 257-265, 1975.
6. Anneroth G,, Eneroth C.M. and Isacsson G. : Crystalline structure of salivary calculi. A microradiographic and microdiffractometric study. J. Oral Pathol., 4(5) : 266-272, 1975.
7. Harrison G.R. : Calculi of salivary gland and duct. Surg. Gy. & Obst., 43 : 431-435, 1926.
8. Doku H.C. and Berkman M. : Submaxillary salivary calculus in children. Am. J. Dis. child., 114 : 671-673, 1967.
9. Levy D.M., ReMine W.H. and Devine K.D. : Salivary gland calculi-pain, swelling associated with eating. JAMA., 181 : 1115-1119, 1962.
10. Seifert G., Miehlike A., Haubrich J, et al. : Diseases of the salivary glands-pathology, diagnosis, treatment, facial nerve surgery. Stuttgart, 1984, Georg Thieme Verg., pp 85-90.
11. Rust T.A., Messerly C.D. and Va WW : Oddities of salivary calculi. Oral surg. Oral med. Oral pathol., 28 : 862-865, 1969.
12. 오치엽, 박하춘, 장승훈, 박영민, 이선철 : 타석의 성분 분석. 한국이비인후과학회지, 29(6) : 821-824, 1986.
13. 이고욱 : 타석의 임상적 고찰, 한국이비인후과학회지, 36 : 2-16, 1993.
14. 김연준, 이승주, 정윤영, 오천환 : 타석에 관한 임상적 고찰. 임상이비인후과지, 4(2) : 326-332, 1993.
15. 변준영, 채요한, 원나경, 이강은 : 악하선계 타석증의 임상적 연구. 임상이비인후과지, 5(2) : 275-280, 1994.
16. 五味武郷 : 本邦における唾石の統計的觀察. 東京醫事新誌, 2750 : 2170-2176, 1931.
17. Ottaviani F., Capaccio P., Campi M. and Ottaviani A. : Extracorporeal electromagnetic shock-wave lithotripsy for salivary gland stones. Laryngoscope, 106(6) : 761-764, 1996.
18. Yoshizaki T., Maruyama Y., Motoi I., Wakasa R. and Furukawa M. : Clinical evaluation of extracorporeal shock wave lithotripsy for salivary stones. Ann. Otol. Rhinol. Laryngol., 105(1) : 63-67, 1996.
19. Kater W., Meyer W.W., Wehrmann T., et al. : Efficacy, risks, and limits of extracorporeal shock wave lithotripsy for salivary gland stones. J. Endourol., 8(1) : 21-24, 1994.
20. Iro H., Schneider H.T., Födra C., et al. : Shockwave lithotripsy of salivary duct stones. Lancet, 30(339) : 1333-1336, 1992.
21. Iro H., Waitz G., Nitsche N., et al. : Extracorporeal piezoelectric shock-wave lithotripsy of salivary gland stones. Laryngoscope, 102(5) : 492-494, 1992.
22. 홍석경, 한병상, 박항 등 : 체외 충격파 쇄석기를 이용한 타석 분쇄에 관한 실험적 연구. 한 이인지, 35(5) : 626-631, 1992.
23. Nahlieli O., Neder A. and Baruchin A.M. : Salivary gland endoscopy. A new technique for diagnosis and treatment of sialolithiasis. J. Oral Maxillofac. Surg., 52 : 1240-1242, 1994.
24. Haring J.I. : Diagnosing salivary stones. J. Am. Dent. Assoc., 122(6) : 75-76, 1991.
25. Som P. M. and Curtin H.D. : Head and Neck

Imaging. 3rd edi., 1996, Mosby-Year Book, Inc., pp 834.
26. Langlais R.P., Langland O.E. and Nortjě C. J. : Diagnostic Imaging of the Jaws. 1st edi., 1995, Williams & Wilkins, pp 626.
27. Blatt I.M., Rubin R., French A.J., et al. : Secretory sialography in disease of the salivary gland. Ann. Otol. Rhinol. Laryngol., 65 : 295-317, 1956.
28. Avrahami E., Englender M. and Chen E. : CT of submandibular gland sialolithiasis. Neuroradiology, 38 : 287-290, 1996.
29. Kurachi Y., Matsumoto H., Nagumo M., et al. : Scanning electron microscopic study of salivary calculi. Jpn. J. Oral Maxillofac. Surg., 26 : 945-951, 1980.
30. Morinaga F. : Scanning electron microscopic observation of the microstructure of salivary calculi. Jpn. J. Stomatol. Soc., 29 : 254-267, 1980.
31. Tohda H., Yamakura K. and Yanagisawa T. : High-resolution electron microscopic study of salivary calculus. J. Electron Microsc. (Tokyo), 44(5) : 399-404, 1995.
32. Kodaka T., Debari K., Sano T. and Yamada M. : Scanning electron microscopy and energy-dispersive X-ray microanalysis studies of several human calculi containing calcium phosphate crystals. Scanning Microsc., 8(2) : 241-257, 1994.
33. Mishima H., Yamamoto H. and Sakae T. : Scanning electron microscopy-energy dispersive spectroscopy and X-ray diffraction analyses of human salivary stones. Scanning Microsc., 6(2) : 487-494, 1992.
34. Yamamoto H., Sakae T., Takagi M. and Otake S. : Scanning electronic microscopic and x-ray microdiffractometric studies on sialolith-crystals in human submandibular glands. Acta Pathol. Jpn., 34(1) : 47-53, 1984.
35. Sakae T., Yamamoto H. and Hirai G. : Mode of occurrence of brushite and whitelockite in a sialolith. J. Dent. Res., 60(4) : 842-844, 1981.
36. Miyake M., Ishii T., Andoh M., et al : Submandibular gland sialolithiasis. Sialographic and pathologic findings with evaluation using SEM and EPMA analysis. J. Nihon Univ. Sch. Dent., 29 : 112-123, 1987.

국문초록

인간 타석의 미세구조적 특징

전북대학교 치과대학 구강내과학교실 및 구강생체과학연구소

김현진 · 이수근 · 서봉직

타석에 관한 연구는 타석증을 보이는 환자에 대한 임상적 특징, 진단 및 치료에서부터 타석의 성분 및 구조 등에 이르기까지 다양한 범위에 걸쳐 이루어지고 있다. 타석의 미세구조에 관한 연구는 타석의 미세구조가 다양한 형태인 것으로 보고되고 있으며, 특히 최근 타석증의 치료에 새롭게 소개되고 있는 체외충격파쇄석술은 타석의 구조에 따라 그 효과가 영향을 받을 수 있을 것으로 사료된다. 이에 저자는 인간 타석의 미세구조에 관한 기본 자료가 필요할 것으로 사료되어 한국인 중년 여성으로부터 적출된 악하선 타석을 광학현미경 및 주사전자현미경을 이용하여 미세구조적 특징을 관찰한 결과, 다음과 같은 결론을 얻었다.

1. 타석은 중심부의 핵, 핵 주변의 층상구조 및 외피막으로 이루어져 있었다.
2. 핵은 비정형의 중심과 상대적으로 균질의 외곽부위로 구성되어 있었다.
3. 핵 주변은 대부분 동심원적인 층상구조를 보였지만 일부분에서는 균질의 구조를 보였다.
4. 타석 단면의 전체직경과 중심부 핵의 직경은 각각 3,500㎛와 1,500㎛였고, 층상구조를 이루는 각 층의 두께는 위치에 따라 약 10-40㎛ 이내였다.

핵심용어 : 타석, 핵, 층상구조, 외피막

LEGEND OF FIGURES

Fig. 1. Occlusal radiograph disclosing an oval stone in Wharton's duct.
Fig. 2. A macrophotograph of the entire view of the sialolith from submandibular gland duct of a female aged 59 years.
Fig. 3. The reflected light microscopic image of the cross-sectioned sialolith (×15).
Fig. 4. The scanning electron microscopic image of the cross-sectioned sialolith (×20).
Fig. 5. The reflected light microscopic image of a central core of the sialolith (×40).
Fig. 6. The scanning electron microscopic image of a central core of the sialolith (×50).
Fig. 7. The reflected light microscopic image of a middle portion of a central core of the sialolith (×70).
Fig. 8. The scanning electron microscopic image of a middle portion of a central core of the sialolith (×1,000).
Fig. 9. The reflected light microscopic image of a lamellar portion of the sialolith (×60).
Fig. 10. The scanning electron microscopic image of a lamellar portion of the sialolith (×80).
Fig. 11. The reflected light microscopic image of a outer surface of the sialolith (×20).
Fig. 12. The scanning electron microscopic image of a outer surface of the sialolith (×80).

논문사진부도 ①

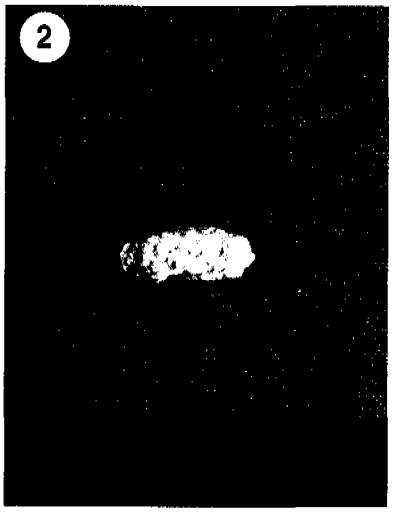

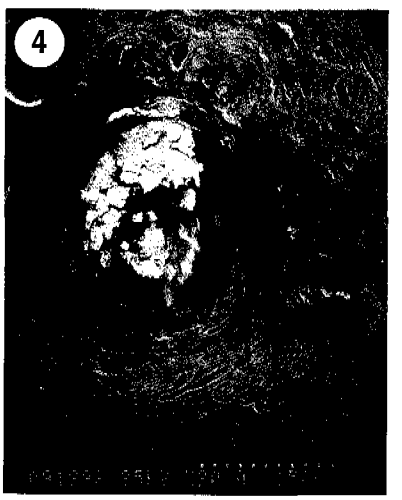

논문사진부도 ②